



An assessment of the process of Self-propagating High-Temperature Synthesis for the fabrication of porous copper composite

A. Moloodi^{a,c}, R. Raiszadeh^{a,*}, J. Vahdati-Khaki^b, A. Babakhani^{b,c}

^a Department of Metallurgy and Materials, Engineering Faculty, Shahid Bahonar University of Kerman, Jomhoori Eslami Blvd., Kerman, Iran

^b Department of Materials Science and Engineering, Engineering Faculty, Ferdowsi University of Mashhad, Azadi Sq., Mashhad, Iran

^c Materials Group, Iranian Academic Center for Education, Culture and Research (ACECR), Mashhad, Iran

ARTICLE INFO

Article history:

Received 30 May 2009

Accepted 25 July 2009

Available online 3 August 2009

Keywords:

Composite materials

Solid state reactions

Metal foam

Porous metals

SHS process

ABSTRACT

The present article describes the process of Self-propagating High-temperature Synthesis (SHS) that is employed for fabricating open cell copper–alumina composite foam. This foam was fabricated by the reactions between the powders of CuO, Al and C. The gas released during these reactions as well as the initial porosity of the green powder compact were suggested to be the sources of the produced pores. Further, the effect of C content and the precursor compressing pressure on the porosity content and morphology of the SHS product was determined. Optical microscopy (OM), scanning electron microscopy (SEM), and X-ray diffraction (XRD) were utilized to characterize the porous samples. The optimum weight fractions for blending the initial powders were determined to be 84 wt.% CuO, 9.5 wt.% Al, and 6.5 wt.% C, and the SHS reaction was sustainable only if the initial compacting pressure of the powders was between 100 and 300 MPa.

© 2009 Elsevier B.V. All rights reserved.

1. Introduction

The foams of certain substances and other highly porous materials that contain a cellular structure are known to possess many interesting combinations of physical and mechanical properties, such as high stiffness in conjunction with very low specific weight or high gas permeability combined with high thermal conductivity [1]. Copper foam is a popular metallic foam that is used in various industrial applications, such as thermal conductors, catalysts, and batteries. The fabrication of porous copper by the process of unidirectional solidification under the effect of hydrogen and the properties of the resultant product were investigated by Nakajima et al. [2] and recently, the Lost Carbonate Sintering (LCS) process was used for the manufacture of open cell copper foams [3,4]. The presence of oxide particles, such as Al₂O₃ in copper would supplement the high thermal properties of the metal with the strength, high chemical and thermal stability of the oxide [5,6]. It was suggested recently that copper–alumina composite foams can be effectively used in laboratory reactors [6,7].

One of the most widely used methods for the manufacture of metal foams, wherein, the shape and size of the cell and the porosity distribution in it can be controlled is based on the techniques

of powder metallurgy. In order to produce aluminum foams, some earlier investigators employed a gas-producing foaming agent, usually TiH₂ [8–10], and recently, the Sintering and Dissolution Process (SDP) [11] was conducted for this purpose.

Another method that can be used for the manufacture of foams of metals is the process of Self-propagating High-temperature Synthesis (SHS). In general, the chemical reactions that synthesize intermetallics or ceramics generate large amounts of heat of reaction [12]. SHS is a process that utilizes these strong exothermic reactions. Once the reaction occurs at the heated zone, the generated heat raises the temperature of the neighboring zone and triggers the reaction again. Hence, the reaction spontaneously propagates throughout the specimen, and results in the formation of bulk intermetallics or ceramics [13], which are generally porous [14]. Intermetallic foams that had an application in surgical implants were successfully manufactured by utilizing the SHS process [15,16].

Under adiabatic conditions, the heat generated by the reaction increases the temperature of the products to a value usually termed as “adiabatic temperature” (T_{ad}). If the heat that is released locally during the reaction is capable of activating the adjacent particles, then the combustion wave would be stable [17]. Merzhanov [18] presented the empirical criterion $T_{ad} \geq 1800$ K for combustion wave stability and Munir and Anselmi-Tamburini [17] proposed an adiabatic temperature of 2000 K as the empirical criterion for a successful SHS reaction. It was also noted that raising the adiabatic temperature would facilitate the SHS reaction. However, only a few stable SHS systems that operate with a T_{ad} of less than 1800 K have been reported in the literature [19].

* Corresponding author. Tel.: +98 9131401488; fax: +98 3412111865.

E-mail addresses: ahmad.moloodi@yahoo.com (A. Moloodi), r.raiszadeh@yahoo.com (R. Raiszadeh), vahdati@um.ac.ir (J. Vahdati-Khaki), babakhni@um.ac.ir (A. Babakhani).

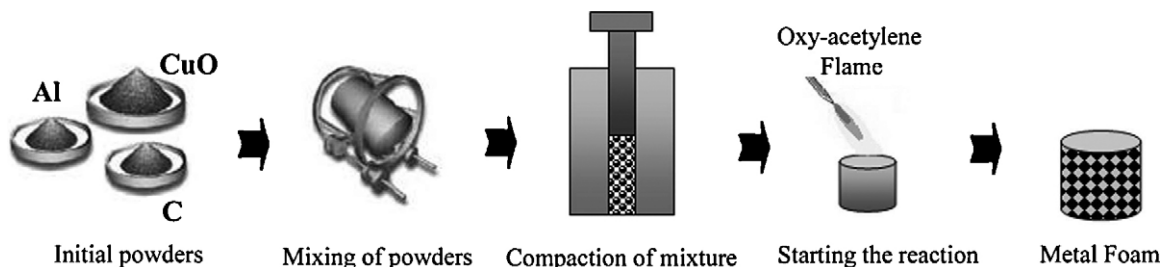


Fig. 1. Schematic illustration of the SHS process implemented to synthesize porous copper–alumina composite.

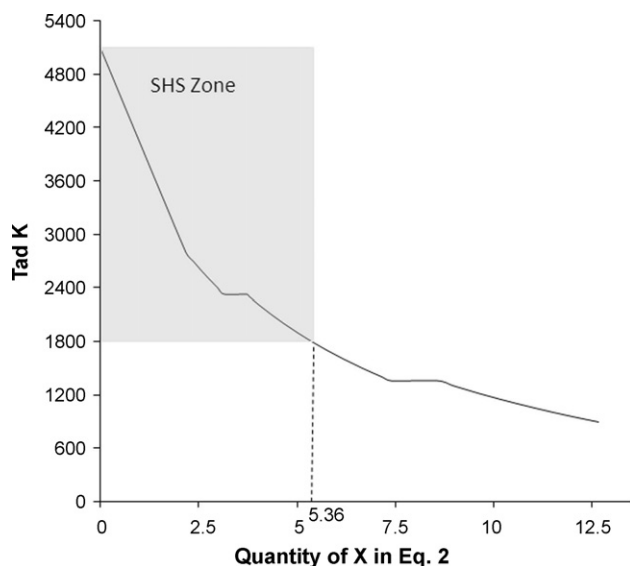


Fig. 2. The relationship between the values of the blending ratio X (in Eq. (2)) and the theoretical adiabatic temperature of the system.

For fabricating the Cu–Al₂O₃ composite, the SHS process works on a principle, which is based on the occurrence of the following thermite reaction [20]:

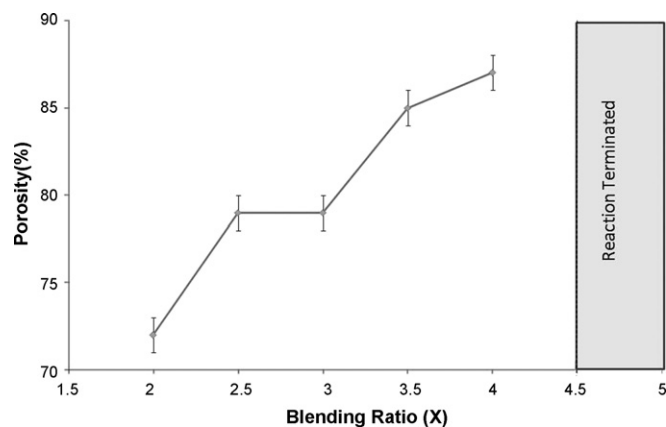
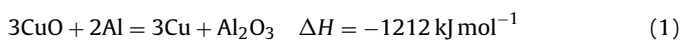
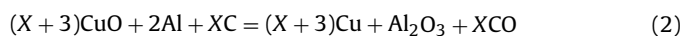


Fig. 4. The porosity content of the specimens synthesized by combustion under different values of blending ratios from $X=2$ to $X=4$.

This reaction emits an enormous amount of heat, and the theoretical adiabatic temperature (T_{ad}) of the system immediately increases to a value of about 5000 K [7]. At this temperature, the products of the reaction would vaporize. Therefore, to decrease this temperature graphite powder is added to the powder mixture, which would also increase the porosity of the final product by producing carbon monoxide gas (Eq. (2)).



The stoichiometric parameter X varies from 0 to 6 in this reaction, signifying the C content ranging from 0 to 35.3 mol% in the

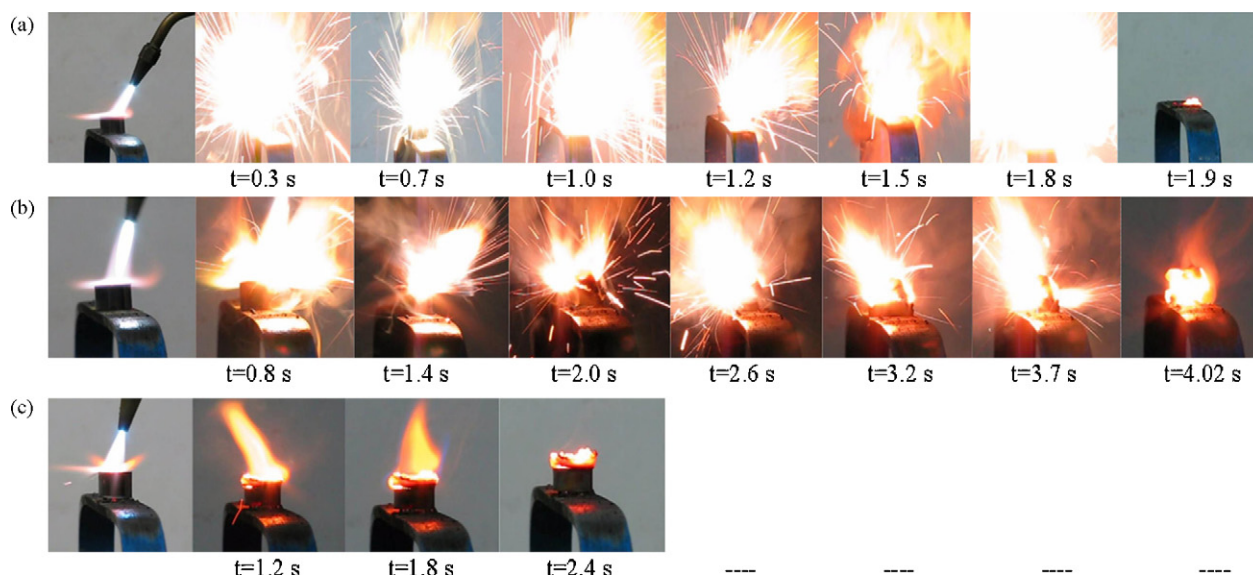


Fig. 3. The recorded images of the combustion reactions of the precursors with blending ratios of (a) $X=0$, (b) $X=3$ and (c) $X=5$.


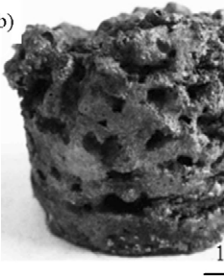
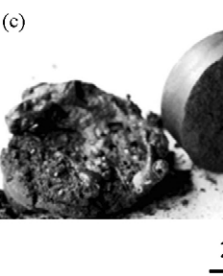
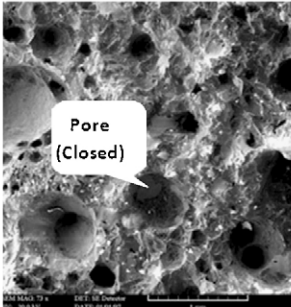
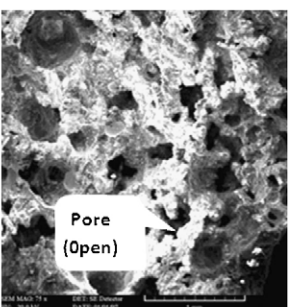
Appearance	(a) 	(b) 	(c) 
Cross-sections			-----
Quantity of X in Eq. 2	X=1	X=3	X=5

Fig. 5. The appearance and the morphology of the pores of the specimens synthesized by combustion under different values of blending ratios of $X = 1, 3$, and 5 .

reactant mixture. Consequently, the temperature of the system will be determined by the value of X in the equation. Fig. 1 shows a schematic outline of the process of SHS implemented to synthesize the porous Cu–Al₂O₃ composite.

Fig. 2 shows the relationship between the values of X and the T_{ad} in the system. Considering the Merzhanov criterion ($T_{ad} \geq 1800$ K) [21], this figure implies that the SHS reaction would be stable, only if the value of X is less than 5.36 .

In the present study, the SHS process was adopted to produce copper–alumina composite foams, in addition, optical and electron scanning microscopy, EDX and X-ray diffraction (XRD) were employed to evaluate the effects of the different blending ratios X and the varied compacting pressures of the green precursor on the

SHS reaction as well as the porosity content and morphology of the final product and the phases formed during the reaction.

2. Materials and methods

Copper oxide (CuO) ($<160 \mu\text{m}$), aluminum ($<45 \mu\text{m}$) and graphite ($<45 \mu\text{m}$) powders were used as the raw materials in the SHS process for the fabrication of the composite foam. First, these powders were evenly blended in a mixer at molar ratios (quantities of X in Eq. (2)) ranging from 0 to 6 . The blended powder was then cold-pressed under different compacting pressures ranging from 90 to 350 MPa in a cylinder ($h = 20$ mm, $ID = 17$ mm) to make a precursor. Further, the top region of the precursor was heated by an oxy-acetylene flame to trigger a combustion reaction. Soon after the completion of the reaction, the cross-section of the specimen was studied using an optical microscope, SEM (Camscan MV2300), which was fitted with an Oxford Inca EDX, and XRD (Philips X-pert). The porosity of the green

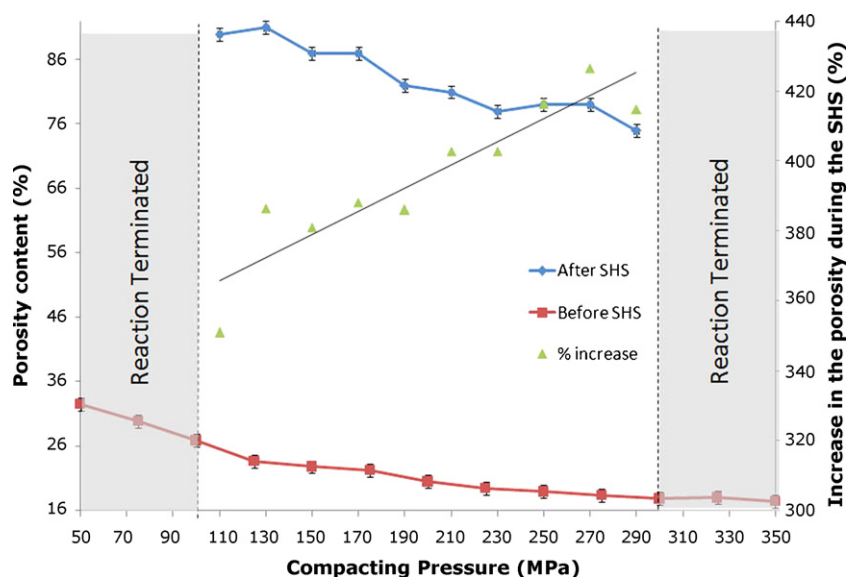


Fig. 6. Porosity of the specimens, the precursors of which were produced under different compacting pressures ($X = 3$), before and after the SHS reaction.

precursor and the synthesized product of the combustion were also measured using the Archimedes method.

Since the main objectives of this stage of the research were the direct observation of the SHS reactions and the study of the characteristics of the products, therefore, no chamber was used to hold the precursor during the reactions.

3. Results

3.1. Evaluation of the SHS reaction, porosity content, and morphology of the pores

The difference noted in the degrees of severity of the reactions that occurred in the different compact samples confirmed that the combustion behavior of the compact reactants varied with the content of C in the initial powder mixture. Fig. 3a illustrates the typical SHS sequence of a compact sample (produced under a compacting pressure of 250 MPa) wherein the molar ratio of CuO:Al:C was 3:2:0 ($X=0$). It is evident that initially upon ignition, a distinct reaction front was formed and then propagated downwards quite harshly in a self-sustaining fashion. The degree of severity of the reaction was excessively high and all the products of the reaction were vaporized. This was attributed to the generation of a high adiabatic temperature during the phase transformation. As also revealed in Fig. 3a, the combustion front traversed the entire sample in about 1.9 s.

The degree of severity of the reaction was moderated by introducing C in the reactant mixture. When the C content increased to 27.3 mol% (CuO:Al:C = 6:2:3 [$X=3$]), as depicted in Fig. 3b, the compact sample almost retained its original shape throughout the SHS process. This implied that the reactions generated a lesser degree of adiabatic temperature in the C-containing compact sample. Moreover, it was noted that the addition of C to the sample also led to a slower propagation of the reaction front. As seen in Fig. 3b, it took about 4.02 s for the combustion wave to reach to the bottom of the sample. On the other hand, Fig. 3c, which illustrates the combustion reaction of a mixture with 33.3 mol% C (CuO:Al:C = 8:2:5

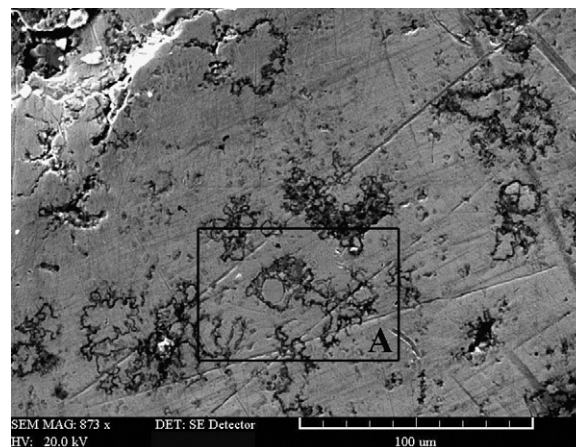


Fig. 7. The secondary electron SEM micrograph of the specimen synthesized by combustion ($X=2$), showing irregular Al_2O_3 particles in a Cu matrix. The EDX elemental map of the area denoted by "A" is shown in Fig. 8.

[$X=5$]), indicates that increasing the amount of graphite to $X=5$ in the reactant mixture caused the SHS process to terminate before its completion. Conducting further experiments with varying C contents from $X=4$ to $X=5$ confirmed a critical C content of $X=4.5$, after which the combustion reaction could not propagate in a sustainable manner. This particular C content (according to Fig. 2) corresponds to an adiabatic temperature of about 2000 K. This criterion for a successful SHS reaction is quite similar to the criterion suggested by Munir and Anselmi-Tamburini [17].

The C content of the precursor also influenced the porosity content and the morphology of the pores that were produced as a result of the reactions. Fig. 4 shows the porosity content of the products, the precursor of which were generated under a compacting pressure of 250 MPa and varied blending ratios that lie between $X=2$ and $X=4$. This parameter controls the fraction of the gaseous phase

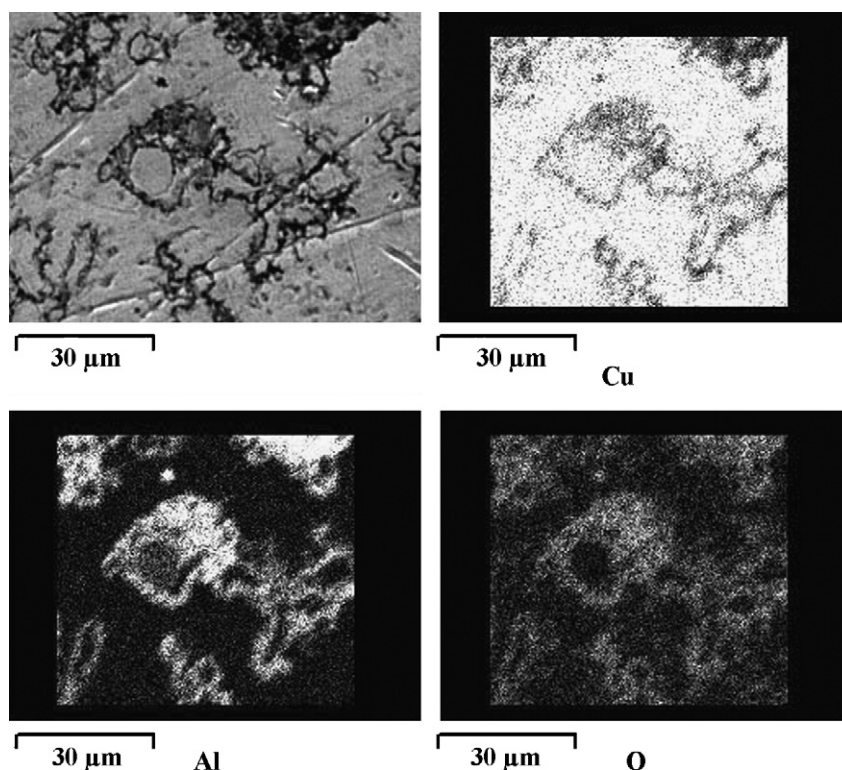


Fig. 8. The EDX elemental map of area "A" given in Fig. 7.

(CO), which influences the formation of porosity during the combustion process, and, as revealed by Fig. 4, the porosity content of the products increased from 72% to 87% due to an increase in the value of the blending ratio from $X=2$ to $X=4$.

Fig. 5 illustrates the appearance and the morphologies of the pores of the Cu–Al₂O₃ foams synthesized by combustion under different blending ratios ($X=1$, $X=3$ and $X=5$). This figure shows that when the C content of the precursor was low ($X=1$, Fig. 5a), the precursor deformed considerably during the SHS process and the pores were produced with a closed morphology, whereas, a precursor with a blending ratio of $X=3$ deformed much less and the morphology of the pores formed during the reaction changed from closed to open pores (Fig. 5b). In addition, as the blending ratio reached to CuO:Al:C = 8:2:5 ($X=5$), the combustion reaction of the compact powder was terminated (Fig. 5c).

3.2. Effect of the compacting pressure

Fig. 6 exhibits the porosity of the specimens (with $X=3$), the precursors of which were compressed under different compacting pressures, before and after the SHS process. According to this figure, as the compacting pressure increased, the porosity content of the precursor before the SHS reaction decreased, first with a greater and eventually with a shallower slope. This can be attributed to the gradual deformation of the powder from a spherical shape to flat grains during compaction, which increased the specific surface area of the powder, and hence, decreased the level of the stress exerted on it, and also the gradual work hardening of the powder grains.

Fig. 6 also shows that an increase in the compacting pressure decreased the porosity content of the specimens after the combustion reaction. This was also observed by Kanetake and Kobashi [15], who attributed it to the lower initial porosity of the precursor under high compacting pressure conditions. However, the relative increase in the porosity of the samples during the SHS process (denoted by triangles) at high compacting pressures was higher than that of the samples with lower compacting pressures.

The precursors that were produced by employing a compacting pressure of less than 100 MPa or greater than 300 MPa were found to be unstable during the combustion, and the SHS process was terminated before its completion.

3.3. The microstructure

Fig. 7 illustrates the secondary electron SEM micrograph of the polished surface of a specimen synthesized by combustion, the precursor of which was produced under a blending ratio of $X=2$ and a compacting pressure of 250 MPa. The EDX studies (Fig. 8) revealed

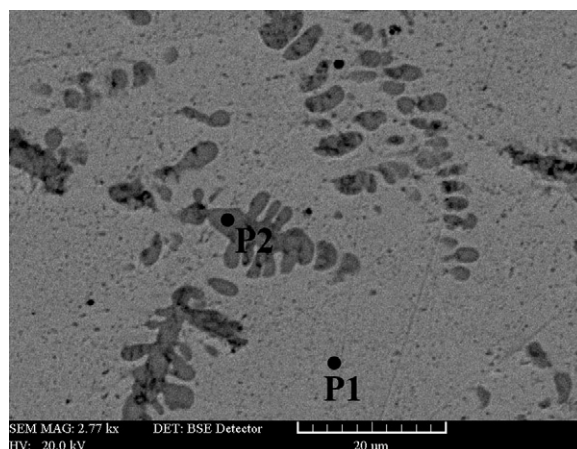


Fig. 9. The back-scattered SEM micrograph of the specimen synthesized by combustion ($X=2$), illustrating Cu₂O dendrites in a Cu matrix. The EDX spectra of points P1 and P2 are shown in Fig. 10.

that the microstructure consisted of irregular Al₂O₃ particles dispersed in a Cu matrix. The back-scattered SEM micrograph of the matrix in a high magnification (Figs. 9 and 10), however, revealed the presence of dendrites of Cu₂O in it. The dendritic morphology of the Cu₂O phase revealed that this phase was formed during the re-solidification of the Cu matrix, which melted under the high reaction heat generated during the SHS process.

The presence of these three phases was also confirmed by the XRD analysis. Fig. 11 illustrates the XRD spectra obtained from the samples under different values of blending ratios that lie between $X=1$ and $X=4$. This figure reveals that with an increase in the blending ratio from $X=1$ to $X=4$, the intensity of the XRD peaks corresponding to Al₂O₃ and Cu₂O phases decreased gradually. The decrease in the intensity of the Al₂O₃ peak was predictable, and in context of Eq. (2), was due to the decrease in the concentration of this phase in the final product under higher values of blending ratios.

4. Discussion

The severe deformation of the precursor under a blending ratio of $X=1$ during the SHS reaction implies that the large amount of heat released during the combustion reaction caused Cu and Al₂O₃ to melt and perhaps Cu to even evaporate, since the high theoretical adiabatic temperature of the reaction (about 3900 K, according to Fig. 2) was above the melting point of alumina (2323 °C) and the boiling point of Cu (2833 °C [20]). The melting of Cu and Al₂O₃ (and

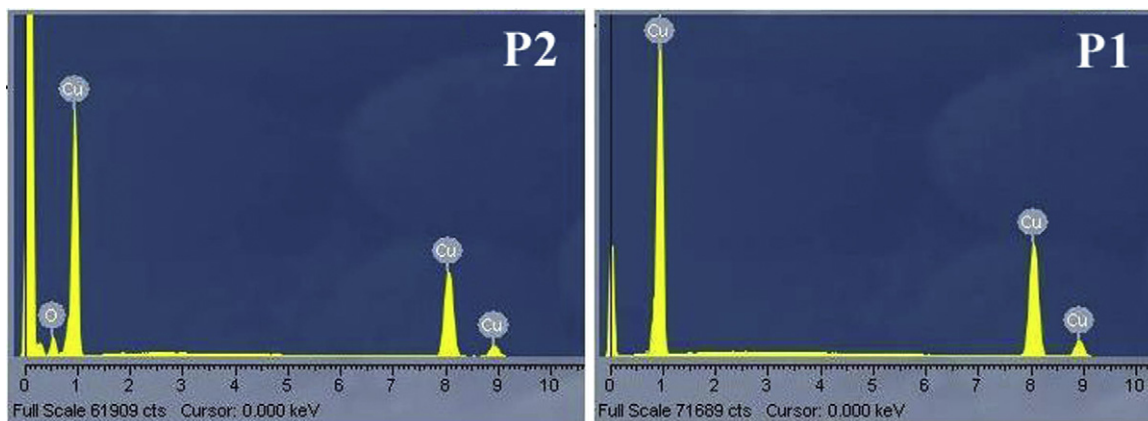


Fig. 10. The EDX spectra of points P1 and P2 given in Fig. 9.

perhaps the evaporation of Cu) were followed by their rapid solidification and condensation due to the low ambient temperature, and as the precursor was not held by a die or inside a chamber, its shape deformed considerably. The absence of ample time for the

produced CO gas to move in the molten matrix caused the pores to appear with a closed morphology.

Raising the blending ratio to $X=3$ increased the amount of the produced CO gas and also caused the theoretical adiabatic temperature to fall to 2300 K. In addition, as the rate of propagation of the reaction front was not very high, the actual temperature at the reaction front should be lower than the theoretical adiabatic temperature, since heat was conducted away from it, but still enough to melt and re-solidify most of the Cu matrix (with a melting point of 1356 K [20]). In this case, the local solidification time at the combustion front was less and the fluidity of the resultant melted Cu was lower than that of the sample with a blending ratio of $X=1$, and hence the shape of precursor deformed to a lesser extent during the SHS process. The higher gas pressure, along with the lower fluidity of the matrix and the shorter solidification time (which limited the flow of the liquid metal to fill the produced pores) increased the porosity content of the sample (see Fig. 4) and changed the morphology of the pores from closed pores to open ones (see Fig. 5).

The final porosity content of the combustion synthesized foam depended on both the porosity content of the green precursor and the porosity that was produced due to the release of the CO gas during the SHS reaction, providing that this gas did not have ample time to escape from the molten matrix before it was solidified.

The change in the green density of the precursor has two opposing effects on the SHS reaction [19,21]. The increase in the green density of the precursor increases the surface contact areas established between the particles, and hence makes the SHS reaction easier. On the other hand, raising the green density of the precursor increases the heat diffusion through the sample. A higher heat diffusivity of the sample causes the temperature at the SHS front to fall, sometimes to less than the critical temperature that is required for a sustainable SHS reaction (i.e., 2000 K in these experiments). The lack of enough surface contact area in the precursors that were generated under a compacting pressure of less than 100 MPa, and the excessive heat diffusivity in the precursors generated by using a compacting pressure of more than 300 MPa, caused the instability and an eventual termination of the SHS reaction in these specimens.

Increasing the compacting pressure at a constant blending ratio of X (Fig. 6) also had a dual opposing effect on the final porosity content of the specimens. This factor, on one hand, decreased the porosity content of the green precursor, which in its turn decreased the porosity content of the product synthesized by combustion. On the other hand, this increased the rate of heat that was conducted away from the reaction zone due to an increase in the level of contact among the precursor powder grains and hence decreased the local solidification time of the molten Cu matrix. The shorter local solidification time decreased the time available for the CO gas to escape from the melt pool and increased the porosity content of the final product. The later effect caused the relative increase in the porosity content of the samples during the SHS process (denoted by triangles in Fig. 6) to increase by raising the compacting pressure, even though, the overall porosity content of the specimens decreased due to the former effect. The results of the XRD analysis (Fig. 11) revealed that the concentration of Cu_2O , which had been produced during the re-solidification of the Cu matrix, decreased in the final product as the blending ratio X increased. This can be explained by considering the binary equilibrium diagram of the Cu–O system (Fig. 12), which shows a eutectic transformation ($L_1 = \text{Cu} + \text{Cu}_2\text{O}$) at 0.43 wt.% O.

Oxygen dissolves in liquid copper (with a standard Gibbs free energy of $-85361.7-18.537T\text{J mol}^{-1}$ [22]), and its solubility increases with an increase in the liquid temperature. According to Fig. 2, increasing the value of the blending ratio X results in a decrease in the adiabatic temperature of the SHS reaction, and hence, a decrease in the amount of oxygen dissolved in the molten Cu, and a decrease in the amount of Cu_2O formed during the

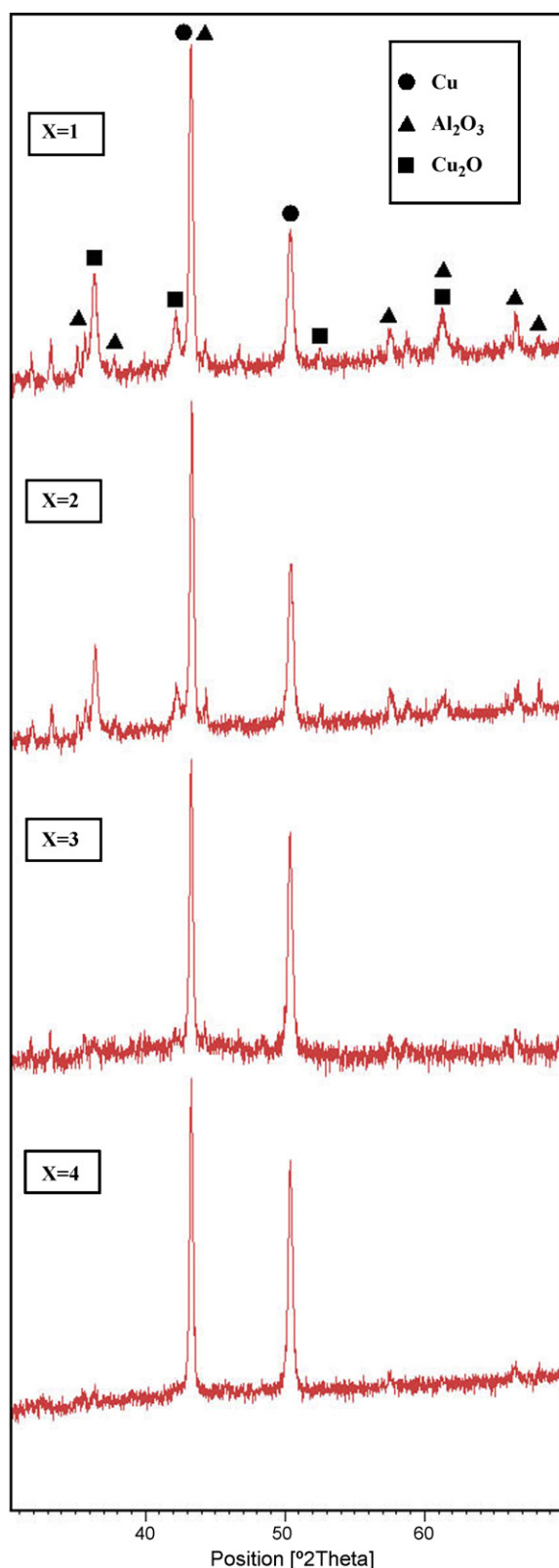


Fig. 11. XRD spectra obtained from the samples under different values of blending ratios that lie between $X=1$ and $X=4$.

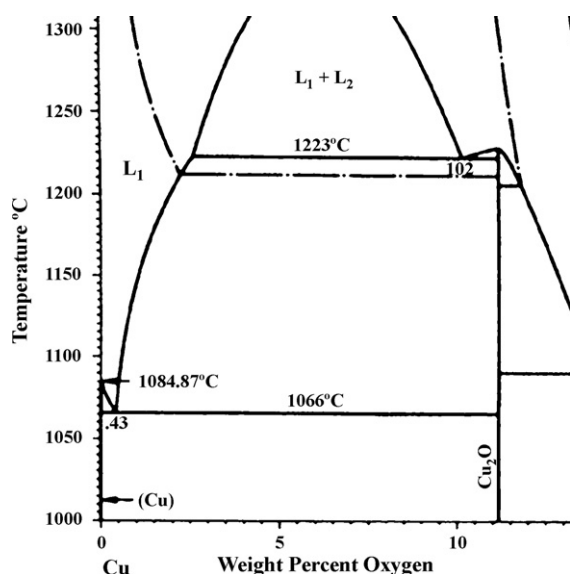


Fig. 12. Binary equilibrium diagram of the Cu–O system, between 0 and 13 wt.% O.

solidification of the copper matrix (see Fig. 12). Another possible explanation is that increasing the value of the blending ratio X increased the amount of the CO gas produced during the combustion reaction (see Eq. (2)). The increase in the amount of CO (a highly reductive gas) caused the concentration of the oxygen that was dissolved in the molten Cu, and hence, the amount of Cu_2O formed during the solidification to decrease.

5. Conclusions

Copper–alumina composite foam was successfully fabricated by the process of Self-propagating High-temperature Synthesis of CuO, Al and C powders, and the following results were obtained:

1. The molar blending ratio of the green ingredients was found to be an important parameter that controlled the behavior of the SHS reaction, the porosity content of the final product, and the morphology of the produced pores. The best molar powder ratio that produced open pores through a sustainable SHS reaction was found to be $\text{CuO}:\text{Al}:\text{C} = 6:2:3$ ($X = 3$).

2. The critical adiabatic temperature, below which the SHS reaction was not sustainable, was determined to be 2000 K (corresponding to $X = 4.5$).
3. The compacting pressure of the powder mixture controlled the porosity content of the final product. The lower the compacting pressure, the greater the porosity of the final product. However, if this pressure was decreased to fall below 100 MPa or increased to rise over 300 MPa, the combustion reaction would not be sustainable and the SHS reaction would be terminated.
4. The SEM and XRD results demonstrated that Cu_2O was formed in the Cu matrix through a eutectic reaction under a low value of the blending ratio ($X < 3$). The concentration of this phase reduced with an increase in the amount of C in the initial powder mixture. This was attributed to the decrease that occurs in the concentration of oxygen dissolved in the molten matrix in higher values of blending ratios.

References

- [1] J. Banhart, Prog. Mater. Sci. 46 (2001) 559–632.
- [2] H. Nakajima, S.K. Hyun, K. Ohashi, K. Ota, K. Murakami, Colloid Surf. A 179 (2001) 209–214.
- [3] A.E. Medhat, K. Saleh, Int. J. Mech. Mater. Des. 4 (2008) 63–69.
- [4] Y.Y. Zhao, T. Fung, L.P. Zhang, F.L. Zhang, Scripta Mater. 52 (2005) 295–298.
- [5] A. Afshar, A. Simchi, Scripta Mater. 58 (2008) 966–969.
- [6] D. Zhongze, F. Hanguang, F. Hanfeng, Q. Xiao, Mater. Lett. 59 (2005) 1853–1858.
- [7] P.K. Jena, E.A. Brocchi, I.G. Solórzano, M.S. Motta, Mater. Sci. Eng. A 371 (2004) 72–78.
- [8] A.R. Kennedy, Scripta Mater. 47 (2002) 763–767.
- [9] E. Koza, M. Leonowicz, S. Wojciechowski, F. Simancik, Mater. Lett. 58 (2003) 132–135.
- [10] M. Guden, S. Yüksel, A. Taşdemirci, M. Tanoğlu, Compos. Struct. 81 (2007) 480–490.
- [11] Y.Y. Zhao, D.X. Sun, Scripta Mater. 44 (2001) 105–110.
- [12] A. Makino, C.K. Law, J. Am. Ceram. Soc. 77 (1994) 778–786.
- [13] M.C. Dumez, R.M. Marin-Ayral, J.C. Tédénac, J. Alloys Compd. 268 (1998) 141–151.
- [14] Z.Y. Fu, H. Wang, W.M. Wang, R.Z. Yuan, J. Mater. Process. Tech. 137 (2003) 30–34.
- [15] N. Kanetake, M. Kobashi, Scripta Mater. 54 (2006) 521–525.
- [16] P. Sevilla, C. Aparicio, J.A. Planell, F.J. Gil, J. Alloys Compd. 439 (2007) 67–73.
- [17] Z.A. Munir, U. Anselmi-Tamburini, in: R. Riedel (Ed.), Handbook of Ceramic Hard Materials, vol. 1, Wiley-VCH, 1999, pp. 322–373.
- [18] A.G. Merzhanov, J. Mater. Process. Tech. 56 (1996) 222–241.
- [19] H. Amel-Farzad, J. Vahdati-Khaki, A. Haerian, A. Youssefi, Solid State Sci. 10 (2008) 1958–1969.
- [20] E.A. Brandes, G.B. Brook, Smithells Metals Reference Book, seventh ed., Butterworth-Heinemann, Oxford, 1999.
- [21] A.D. Bratchikov, A.G. Merzhanov, V.I. Itin, V.N. Khachin, E.F. Dudarev, V.E. Gyunter, V.M. Maslov, D.B. Chernov, Powder Metall. Met. C+ 19 (1980) 5–8.
- [22] ASM Handbook: Casting, vol. 15, 10th ed., ASM International, 1990.